Article

pubs.acs.org/Biomac

Calcium-Triggered Pulsatile Delivery of Parathyroid Hormone from Microbeads for Osteoporosis Treatment

Min-Kyoung Kim,[#] Ha Neul Lee,[#] Ratchapol Jenjob, Junghan Lee, and Su-Geun Yang*

WCSL, Department of New Drug Development, Inha University College of Medicine, B-308, Chungsuk Bldg, 366, Seohae-Daero, Jung-Gu, Incheon 22332, Republic of Korea

Supporting Information

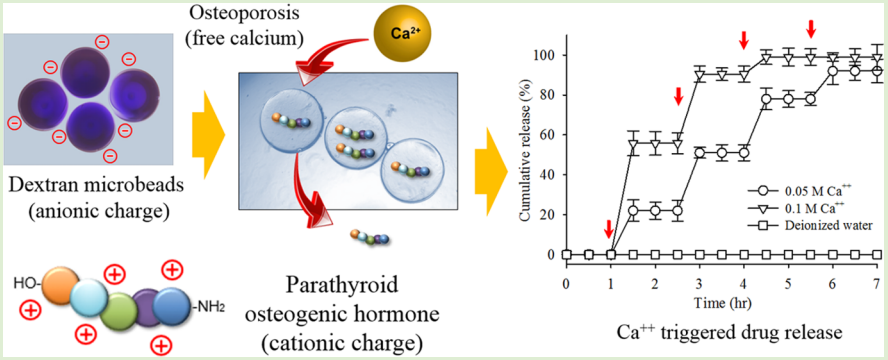

ABSTRACT: Recombinant human parathyroid hormone 1-34 (rhPTH 1-34) is the most potent anabolic drug recommended for patients with osteoporosis who do not respond to conventional treatment. However, subcutaneous intermittent injection is the only effective regimen due to its unusual action of mechanism. This regimen is inconvenient and is a big hurdle in clinical applications. In this study, we designed polyelectrolyte microbeads that can deliver rhPTH 1-34 in response to Ca^{2+} concentration, which indicates the osteoporotic status. Dextran photopolymer was synthesized, mixed with anionic monoacrylate, and photopolymerized by passing through capillary microfluidics to obtain the microbeads. The anionic property of microbeads was confirmed by toluidine blue staining. One microbead, loaded with a 1 day dose of rhPTH 1-34 (23.4 ± 0.9 μg), released rhPTH 1-34 in a triggered manner following the addition of Ca^{2+} ion. In vitro cell study demonstrated that rhPTH 1-34 released in a pulsatile manner from the microbeads induced osteogenic markers (ALP, RUNX2, and OPN) and precipitated mineral disposition more effectively.

1. INTRODUCTION

Osteoporosis is a systemic disorder characterized by micro-architectural deterioration of bone tissue, leading to bone fragility and increased susceptibility to fractures of the hip, spine, and wrist. In 2015, the global drug market for osteoporosis was estimated at USD 11.20 billion and is expected to expand to USD 14.30 billion by 2021. Most drugs for osteoporosis (bisphosphonates, calcitonin, and estrogen receptor modulators) suppress bone loss rather than promoting bone formation.[1] rhPTH 1-34 is the only anabolic peptide drug that stimulates bone formation by activating osteoblasts and inhibiting osteoclasts.[2,3] Currently, daily subcutaneous injection is the only available means of administration of rhPTH 1-34. A sustained delivery system is the best solution for peptides or hormones that have a short biological half life and need to be injected daily or more. However, rhPTH 1-34 possesses erratic biological properties. The continuous release treatment of rhPTH 1-34 leads to catabolic degradation of bone tissues; only the intermittent treatment is effective for osteoporosis.[4,5] Therefore, the development of a more functional delivery system that can exert the complete therapeutic potential of rhPTH 1-34 is a big challenge. Recently, Langer et al. reported a successful clinical study on a rhPTH1-34 loaded microchip that can release the drug intermittently by wireless control.[6] However, this system requires invasive surgical implantation, which is a large barrier for wide clinical application.

In the study, we designed a pulsatile delivery system of rhPTH 1-34 that can release the drug in response to free calcium concentration, which reflects the bone loss in the body. Functional anionic polyelectrolyte microbeads were fabricated under capillary microfluidic and photocrosslinking conditions. Polyelectrolytes are macromolecules that possess a repeating electrolyte group (polycations or polyanions). One of the beneficial properties of polyelectrolytes is that they easily form a complex with oppositely charged molecules.[7−10] Michaels et al. first reported that counter-charged polyelectrolytes interact to form spherical complexes.[8] Recently, multilayered micro-capsules, fabricated by the sequential adsorption of counter-charged polyelectrolytes, have been widely studied for the delivery of active agents, nucleotides, proteins, drugs, and

Received: May 30, 2017
Revised: August 22, 2017
Published: August 29, 2017

DOI: 10.1021/acs.biomac.7b00750
Biomacromolecules 2017, 18, 3099−3105

Scheme 1. Ionic Absorptive Loading of Cationic Human Parathyroid Hormone (rhPHH 1-34) on the Sulfonic-Acid-Functionalized Anionic Dextran Microbeads and Osteoporotic Ca^{2+}-Triggered Drug Release

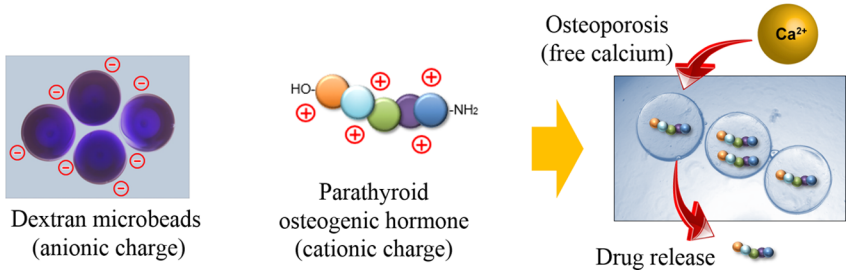

Scheme 2. Fabrication of Anionic Polyelectrolyte Microbeads[a]

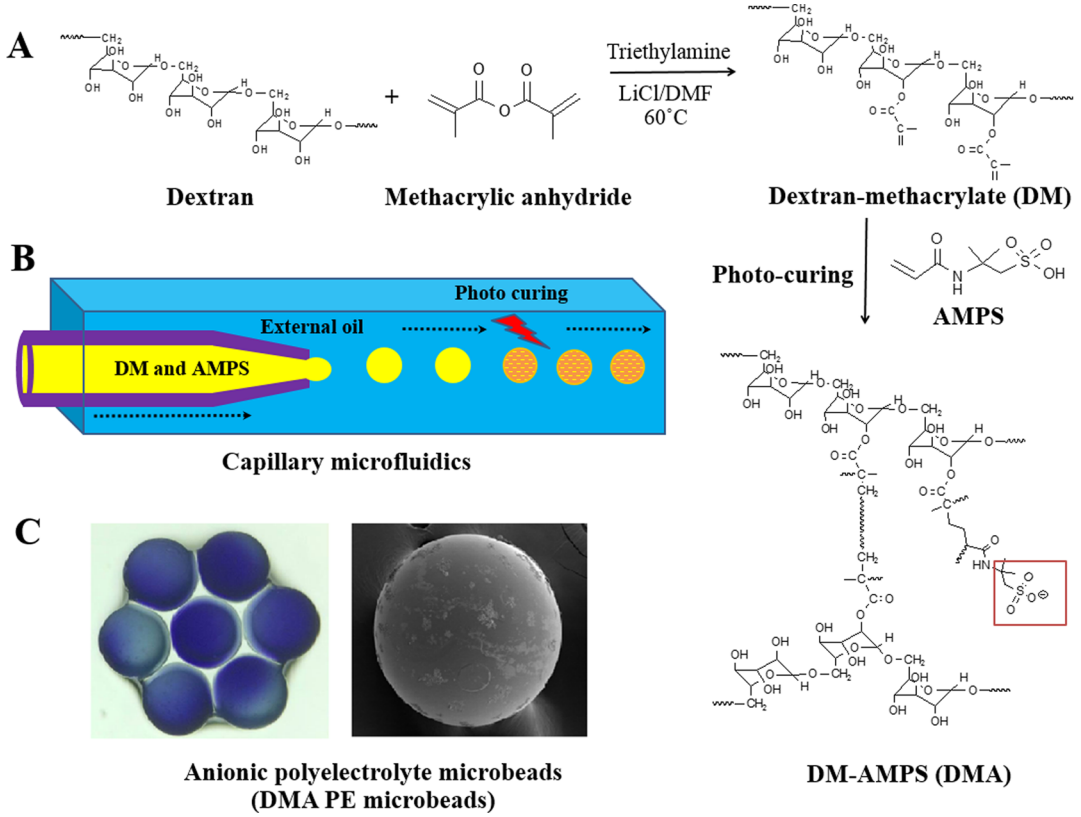

[a](A)Synthesis of dextran-based photocrosslinking polymer (dextran-mathacrylate; DM) and introduction of anionic monomer (2-acrylamido-2-methylpropane sulfonic acid; AMPS) during the photo-polymerization of microbeads. (B) Capillary microfluidic and photo-curing formation of microbeads. (C) Optical microscopic and SEM observation of anionic polyelectrolyte microbeads (DMA PE microbeads).

viruses.[11−14] Crespy and his research group applied polyelectrolyte nanocomplex for the delivery of antiobesity peptide drug. pH-dependent release of antiobesity peptide suggested the potential application of polyelectrolyte for the delivery of peptide drug in the body.[15]

We report a one-step photocrosslinking fabrication method for polyelectrolyte microbeads using capillary microfluidics. Dextran methacrylate (DM), a photocrosslinking polymer, was synthesized, mixed with anionic photocrosslinking monomer acrylamido-2-methylpropanesulfonic acid (AMPS), and introduced to capillary microfluidics. While passing through the capillary microfluidics, droplets of polyelectrolytes solution formed, which were photopolymerized under UV light to obtain polyelectrolyte microbeads (dextran methacrylate−AMPS polyelectrolyte microbeads; DMA PE microbeads). Consequently, the functionalities of DMA PE microbeads as a pulsatile release drug carrier of rhPTH 1-34 (Scheme 1) were evaluated by cationic drug absorption, in vitro release, and cellular studies.

2. MATERIALS AND METHODS

2.1. Materials. Dextran (70 kDa), methacrylic anhydride (MA, 94%), irgacure 2959 (98%), toluidine blue O, 2-acrylamido-2-methylpropanesulfonic acid (AMPS, 99%), L-ascorbic acid (≥98%), *β*-glycerophosphate (≥99%), Span 20, and dexamethasone bioreagent (≥97%) were purchased from Sigma-Aldrich (St. Louis, MO). rhPTH 1-34 was obtained from Bachem California. Triethylamine (TEA), *N*,*N*-dimethylformamide (DMF, >98%)) and lithium chloride (LiC, > 98.2%)) were purchased from DAIHAN scientific (Wonju, Gangwon, Korea). Medium-chain triacylglyceride (MCT) oil was obtained from Nisshin Oililo Group (Shinkawa, Tokyo, Japan).

2.2. Synthesis of Photocrosslinking Polymer. Dextran (1.6 g, 10 mmol) was dissolved in the LiCl/DMF (1.0 wt %) at 90 °C. After

DOI: 10.1021/acs.biomac.7b00750
Biomacromolecules 2017, 18, 3099−3105

the dextran was completely dissolved, the temperature of solution was set at 60 °C. TEA (1.4 mL, 10 mmol) as a catalyst was injected into the dextran solution and stirred for 15 min. Methacrylic anhydride (MA, 496 μL, 5 mmol) was slowly added to the reaction flask. The reaction was performed at 60 °C for 10 h under stirring at 600 rpm (Scheme 2A). After completion of the reaction, the product was precipitated using cold isopropyl alcohol and washed several times with isopropyl alcohol using the centrifugation technique. The sample was purified using a dialysis membrane (Thermo Scientific MWCO 13 kDa, Waltham, MA) for 2 days. Purified Dex-MA was lyophilized and stored at room temperature until use. The conjugation of MA with dextran was confirmed by ^{1}H NMR (Figure S1). The protons in methacrylate vinyl groups appeared at 5.6 and 6 ppm (Figure S1C) and the MA methyl protons at 1.9 ppm. The degree of substitution, determined by the ratio of the integral of MA protons at ∼5.6 and ∼6 ppm to that of dextran at ∼5 ppm, was calculated to be 32.2%.[16,17] FTIR was employed to analyze the carbonyl and double-bond groups after modification of MA on dextran. The appearance of C═O peak at 1715 cm^{-1} and C═C band at 1638 cm^{-1} of methacrylic fragments of MA indicated successful conjugation between MA and dextran (Figure S2).[18]

2.3. Capillary Microfluidic Preparation of Anionic Polyelectrolyte Microbeads. The microfluidic device was fabricated by assembling pulled glass capillary tubes (outer diameter: 1 mm; inner diameter: 0.58 mm; pulled tip diameter: 250 μm, 1B100-6, World Precision Instruments, Sarasota, FL). The cross-linking of DM-AMPS under UV light was performed as follows (Scheme 2A,B): 200 mg of DM powder or 40 mg of AMPS was dissolved in 1 mL of 0.2 wt % irgacure 2959 (water phase). Medium-chain triglyceride (MCT) oil containing 0.1% span 20 was used as the oil phase. The flow rate of water and oil phase was 30 and 300 μL min^{-1}, respectively. A syringe injector was used for the water and oil phase. The W/O emulsion droplets were produced at the tip of a capillary. The emulsion droplets were polymerized to form microbeads (Scheme 2C) under UV light (80 W). The obtained polyelectrolyte microbeads were washed with 70% ethanol several times and kept in 70% ethanol overnight for dehydration. The surface morphology of polyelectrolyte microbeads was examined by scanning electron microscopy (SEM; S800, Hitachi, Tokyo, Japan). The polyelectrolyte microbeads were dried at room temperature overnight. The dried samples were attached to an aluminum stub and coated with platinum. The coated samples were observed on SEM at 15 kV.

2.4. Toluidine Blue O Staining of DMA PE Microbeads. Toluidine blue O (TBO) is a cationic metachromatic blue dye with high affinity for acidic substances. The color shift of TBO, from blue to red-violet, after binding with counterions suggests the presence of free electronegative groups in the substance. DMA PE microbeads were stained with 200 μL of 0.1 mM TBO by incubated shaking for 2 h and washed with distilled water. The color of polyelectrolyte microbeads was observed using the optical microscope (ZEISS Stemi 508, Oberkochen, Germany).

2.5. Loading of rhPTH 1-34 on DMA PE Microbeads. rhPTH 1-34 was labeled with FITC, and the adsorption of FITC-rhPTH 1-34 on the polyelectrolyte microbeads was observed using a fluorescence microscope. rhPTH 1-34 (0.25 mM) and FITC-NHS (0.3 mM) were dissolved in 0.5 mL of dimethyl sulfoxide separately. After being dissolved, the solutions were mixed and stirred at room temperature in the dark for 2 h. The synthesized FITC-rhPTH 1-34 was precipitated with cold acetone and centrifuged at 5000 rpm for 20 min at 4 °C. Dextran methacrylate microbeads (DM microbeads), made without the introduction of AMPS for negative control test, and DMA PE microbeads were immersed in FITC-rhPTH 1-34 solution. After washing, the microbeads were observed using a microscope. The loading of rhPTH 1-34 on the DMA PE microbeads was evaluated as follows. rhPTH 1-34 solution (1 or 2 mg) was added to ∼80 EA of DM microbeads and DMA PE microbeads and maintained at 4 °C for 7 h. At a predetermined time, the sample solution was extracted and filtered through a syringe filter (0.45 μm, SmartPor-ll, SmartMembranes, Halle, DE). The concentration of free rhPTH 1-34 in sample solution was measured by HPLC (Waters 2610 system, Milford, MA) according to a previously described method.[19] The amount of drug adsorption was calculated as follows.

$$\text{drug loading}\left(\frac{\mu g}{\text{microbead}}\right) = \frac{W_{\text{drug total}} - W_{\text{free drug}}}{\text{number of microbeads}}$$

2.6. In Vitro Release of rhPTH 1-34 from DMA PE Microbeads. In vitro release of rhPTH 1-34 from DMA PE microbeads was estimated as follows. rhPTH 1-34 (1 mg) was loaded on 80 DMA PE microbeads by mixing and resuspended in 1 mL of release medium after washing with fresh distilled water and horizontally shaken at 4 °C. Release medium (200 μL) was extracted at intervals and replaced with an equal amount of fresh medium. Intermittent release study of rhPTH 1-34 was performed by adding 200 μL of $CaCl_2$ solution. The amount of released rhPTH 1-34 was measured by HPLC (Waters 2610 system, Milford, MA).

2.7. MC3T3-E1 Cell and OCCM-30 Cell Culture. Two bone cell lines were used in this study. MC3T3-E1 cells (murine osteoblast cell line), appropriate for osteoblast studies, were selected for bone formation marker study. OCCM-30 cells are cementoblasts cell lines that play a central role in periodontal development and regeneration and used to estimate the degree of mineralization (Alizarin Res S staining study).

Cells were plated in six-well dishes at a density of 1 × 10^5 cells/well grown in modified minimum essential medium (Hyclone α-MEM, Pittsburgh, PA) containing 10% v/v fetal bovine serum (FBS) with 1% antibiotics. Cells were incubated at 37 °C with 5% CO_2. The media were changed every 2 days. Mineralization solution containing ascorbic acid (50 μM), dexamethasone (100 nM), and β-glycerophosphate (10 mM) (Sigma, St. Louis, MO) was added to the culture media when the degree of mineralization was estimated.

2.8. Cellular and Tissue Toxicity of DMA PE Microbeads. Cellular toxicity of DMA PE microbeads was evaluated against MC3T3-E1 cells. Cells were seeded to 24-transwell plates at 1.5 × 10^5 cells/well and incubated for 24 h. The DMA PE microbeads were located on the upper side of transwell plates and incubated together with cells. After 24 h of incubation, the microbeads were removed and 10 μL of WST-1 and 100 μL of the cell solution were added to wells and incubated for an additional hour. Cell viability was measured at 450 nm using a microplate reader (Infinite 200 PRO, Männedorf, Switzerland). Cytotoxicity of the DMA PE microbeads was calculated as percentage cell viability (measured as WST-1 reduction) compared with the control.

To evaluate tissue toxicity, the DMA PE microbeads were injected into rat leg muscles. Saline was subcutaneously inoculated at the same area for comparison. Two weeks after implantation, the specimens were recovered, fixed with 10% buffered formalin, and embedded in paraffin. Samples were sliced into 3 μm thick sections, which were stained with hematoxylin and eosin and observed under a microscope (ZEISS Stemi 508, Oberkochen, Germany).

2.9. Mineralization Nodule Staining. The degree of mineralization during the intermittent treatment with rhPTH 1-34 (DMA PE microbeads) was observed by alizarin red S staining method. OCCM-30 cells were treated with rhPTH 1-34 or vehicle mineralization solution for 3 days after seeding on the bottom side of the transwell plate and cultured in mineralization solution without rhPTH 1-34 for 7 days.

rhPTH 1-34 (50 ng/mL) was dissolved in the mineralization solution and used for the continuous treatment (control group). For the intermittent treatment, DMA PE microbeads were located on the upper side of transwell plates, and the release was triggered by adding $CaCl_2$ solution. Control group was also treated with the $CaCl_2$ solution.

2.10. Estimation of Osteoblast Differentiation Markers. MC3T3-E1 cells were used for the study and treated with DMA PE microbeads. The intermittent treatment was performed following the same methods described in Section 2.9. The treatment time was fixed at 6 h of each 48 h period. After treatment, the medium was replaced with fresh medium. At the end of the experiments, cells were recovered for the next study. Osteoblast differentiation was confirmed

DOI: 10.1021/acs.biomac.7b00750
Biomacromolecules 2017, 18, 3099−3105

by qRT-PCR using marker genes, that is, RUNX2, ALP, and OPN in MC3T3-E1 cells. The samples were normalized using glyceraldehydes-3-phosphate-dehydrogenase (GAPDH). The experiments were repeated thrice for each sample. qRT-PCR was performed according to the published kit protocols. Mouse-specific primers were designed and synthesized by M.biotec (Seoul, Korea). Total RNA was extracted using TRIsure (Bioline, BIO-38033, U.K.) following the manufacturer's instructions. Total RNA (1 μg) was subjected to reverse transcription polymerase chain reaction (RT-PCR) amplification using the Tetro cDNA Synthesis kit (Bioline, BIO-65043, U.K.). Complementary DNA (cDNA) was synthesized by reverse transcription at 45 °C for 30 min, followed by reverse transcriptase inactivation at 85 °C for 5 min. SYBR green (M.biotech, 18302, South Korea) was used in RT-PCR quantification. The thermal cycling profile comprised stage 1 (95 °C for 10 min) and stage 2 (95 °C for 15 s, followed by 58 °C for 1 min). Stage 2 was repeated for 40 cycles. The primers used are shown in Table S1.

3. RESULTS AND DISCUSSION

3.1. Microfluidic and Photocrosslinking Fabrication of Polyelectrolyte Microbeads. In this study, we demonstrated the one-step photocuring fabrication of polyelectrolyte microbeads using the capillary microfluidic photocrosslinking method (Scheme 2). Photopolymer (dextran methacrylate; DM) was synthesized, mixed with anionic photocrosslinking monomer AMPS, and photopolymerized by passing through capillary microfluidics. Photopolymerization between DM and AMPS allows one-step formation of anionic spherical microbeads. The modification of dextran with MA, illustrated in Scheme 2A, was confirmed by ^{1}H NMR and FTIR (Figures S1 and S2). The introduction of AMPS to microbeads was confirmed by FTIR (Figure S3). The size of microbeads observed by SEM was ~785 μm with monodispersed and spherical shapes. After drying at room temperature, the average size of DM and DMA microbeads decreased from 785 to 458.7 ± 28.7 μm, respectively, due to dehydration (Figure 1).

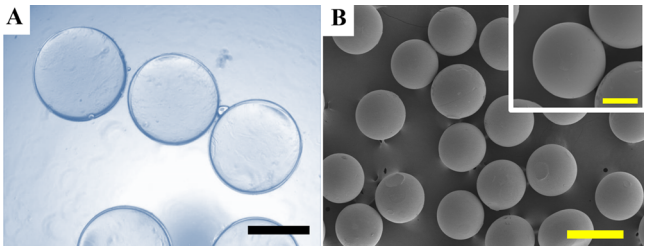

Figure 1. (A) Optical images of DMA PE microbeads in swelling state; scale bar represents 500 μm. (B) SEM observation of DMA PE microbeads in dry state; scale bar represents 500 μm and scale bar in insert represents 200 μm.

3.2. Loading of rhPTH 1-34 on DMA PE Microbeads. The photopolymerization of AMPS with dextran methacrylate introduced the anionic property to microbeads and allowed active absorption capacity against cationic rhPTH 1-34 (pK_a = 8.77). To prove the existence of a negative charge on the DMA PE microbeads, TBO test was performed. TBO, a typical cationic dye, can be adsorbed on the anionic microbeads and changes color from blue to red-violet.[20,21] Figure 2A shows that DM microbeads exhibited blue color, whereas DMA PE microbeads turned violet, indicating the anionic properties of microbeads. FTIR spectrum of DMA sample confirmed the presence of AMPS at 1550 cm^{-1}, corresponding to N−H of AMPS depicted in Figure S3.

The actual loading of rhPTH 1-34 on DMA PE microbeads was observed using a fluorescence microscope. For the study, fluorescence-labeled rhPTH 1-34 (FITC-rhPTH 1-34) was synthesized, loaded on DMA PE microbeads. Figure 2B1,B3 shows DMA PE microbeads before and after the drug loading, respectively. The color of DMA PE microbeads changed to fluorescent aquamarine after the loading of FITC-rhPTH 1-34 (Figure 2B4), whereas a dark color was observed before the loading (Figure 2B2).

The loading amount of rhPTH 1-34 on the polyelectrolyte microbeads was measured three times. Figure 3A demonstrated that drug loading increased to 22.1 ± 3.4 μg per microbead within 30 min and gradually increased to 31.5 ± 0.9 μg at 7 h. Meanwhile, the drug loading of DM microbeads (negative control) was 9.6 ± 3.5 μg (Figure 3B).

Our results showed that rhPTH 1-34 was actively loaded on the DMA PE microbeads. The isoelectric point of rhPTH 1-34 is 8.77, suggesting that rhPTH 1-34 remains in the cationic form at the biological pH. Therefore, rhPTH 1-34 can be loaded on DMA PE microbeads through electrostatic interaction between cationic rhPTH 1-34 and negatively charged AMPS. The results are presented in Figures 2 and 3, which clearly support the hypothesis that the negatively charged AMPS aided the binding of rhPTH 1-34. Considering that the therapeutic daily dose of rhPTH 1-34 is 20 μg, we concluded that DMA PE microbeads have sufficient drug-loading capacity for the delivery of rhPTH 1-34.[22]

3.3. Ca^{2+} Ion-Triggered Pulsatile Release of rhPTH 1-34. rhPTH 1-34 is a recombinant form of parathyroid hormone. Subcutaneous injection is the only available form in the clinics. Clinical reports prove that continuous treatment with rhPTH 1-34 activates osteoclasts rather than osteoblasts and promotes bone lysis rather than bone formation.[4,5] These clinical data suggest that a pulsatile delivery system is required for rhPTH 1-34. In this study, we observed calcium-triggered release of rhPTH 1-34 from the DMA PE microbeads (Scheme 1). The release of the drug was triggered by the addition of $CaCl_2$ solution in the sample collection step. As shown in Figure 4, DM microbeads released all of the loaded rhPTH 1-34 at once, whereas DMA PE microbeads showed a pulsatile release pattern upon the addition of $CaCl_2$ solution. The total amount of rhPTH 1-34 released from DMA PE microbeads was around 30.0, 36.6, and 16.3 μg after the first, second, and third cycles of Ca^{2+} treatment, respectively (data not shown).

We observed that the concentration of $CaCl_2$ solution affected the release rate of rhPTH 1-34. Higher concentrations of $CaCl_2$ solution resulted in higher release (Figure 5). With 0.1 M $CaCl_2$ solution as the medium (Figure 5, triangle line), 58.8% of the loading amount of rhPTH 1-34 was released after the first treatment. However, 0.05 M $CaCl_2$ solution resulted in the release of 30.0% of the loading dose after the first treatment. When distilled water was used as the medium, no rhPTH 1-34 was released from the DMA PE microbeads for 7 h.

These results revealed that Ca^{2+} triggered the release of rhPTH 1-34, and the release can be controlled in pulsatile manner (Figures 4 and 5). On the basis of the results, we propose that our system can act as a pulsatile delivery system of rhPTH 1-34 in the treatment of osteoporosis. The increased osteoclast activity may enhance the release of free calcium from the bone, and the increased local concentration of free calcium may trigger the release of rhPTH 1-34 from the microbeads.

DOI: 10.1021/acs.biomac.7b00750
Biomacromolecules 2017, 18, 3099−3105

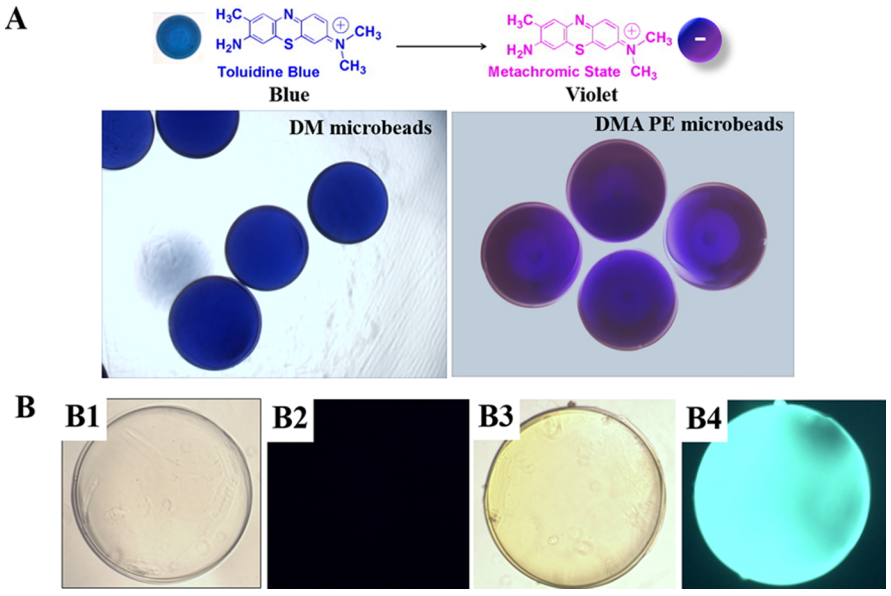

Figure 2. (A) Ionic absorptive loading of cationic dye (toluidine blue O) by DM microbeads (negative control) and anionic DMA PE microbeads. Anionic DMA PE microbeads absorbed cationic toluidine blue O and changed color to violet. (B) Loading of FITC-rhPHH 1-34 onto DMA PE microbeads. DIC images before (B1) and after adsorption (B3); fluorescence phase images before (B2) and after adsorption (B4).

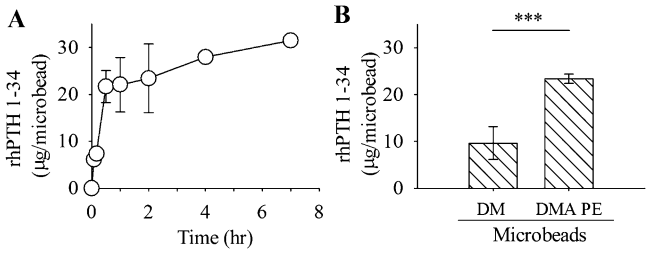

Figure 3. (A) Adsorption profile of rhPTH 1-34 onto DMA PE microbeads. (B) Adsorption capacity of DM microbeads and DMA PE microbeads. DMA PE microbeads absorbed more than 2.5 times the amount of rhPTH 1-34 compared with DM microbeads in 30 min. Experiments were performed in triplicate (mean ± S.D., *** P < 0.001).

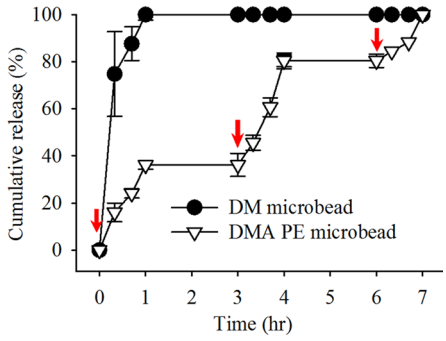

Figure 4. Ca^{2+} ion-triggered pulsatile release of rhPTH 1-34. Cumulative release profile of rhPTH 1-34 from DMA PE microbeads under Ca^{2+} ions triggering and DM microbeads. Release of rhPTH 1-34 from DM microbeads was performed without Ca^{2+} ions triggering (mean ± S.D.).

3.4. Cellular and Tissue Toxicity of DMA PE Microbeads. The WST assay against MC3T3-E1 cell was used to study the cytotoxicity of DMA PE microbeads. We postulated that Ca^{2+} ions had an effect on the release of rhPTH 1-34 from the polyelectrolyte microbead through ion exchange. Therefore,

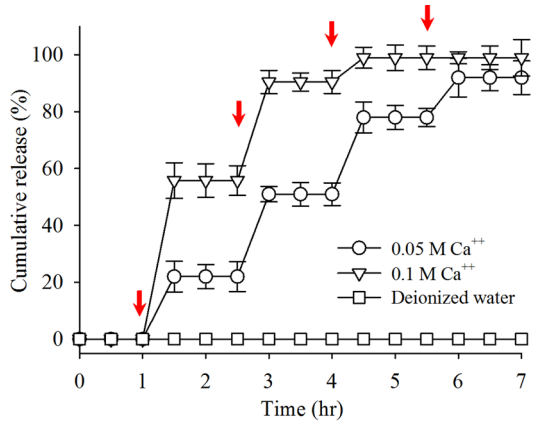

Figure 5. Cumulative release of rhPTH 1-34 from DMA PE microbeads under different concentration of Ca^{2+} ion triggering.

Ca^{2+} ions were tested at various concentrations for cytotoxic effects. Figure 6A shows relative cell viability during 75 h of incubation of Ca^{2+} and polyelectrolyte microbeads. Compared with the control cells (no Ca^{2+} added, 0 mM), Figure 6A showed nonsignificant reduction in the cell viability in 1.5, 6.25, and 25 mM concentration of Ca^{2+}-treated cells. There was no observed cytotoxicity of Ca^{2+} ions and the microbeads. Tissue toxicity, observed after intramuscular injection of DMA PE microbeads, suggested that DMA PE microbeads could be used as drug carriers without severe tissue toxicity (Figure 6B). A slight or moderate inflammation-related fibrosis was observed around the microbeads 7 days after the muscular injection.

3.5. Induction of Bone Formation Markers. The expression of bone formation markers such as runt-related transcription factor 2 (RUNX2), alkaline phosphatase (ALP), and osteopontin (OPN) was analyzed in preosteoblast (MC3T3-E1) (Figure 7). The bone formation markers in the continuous treatment and the pulsatile rhPTH 1-34 treatment using DMA PE microbeads were compared in this experiment. After the treatments, the expression of all of the markers was

DOI: 10.1021/acs.biomac.7b00750
Biomacromolecules 2017, 18, 3099−3105

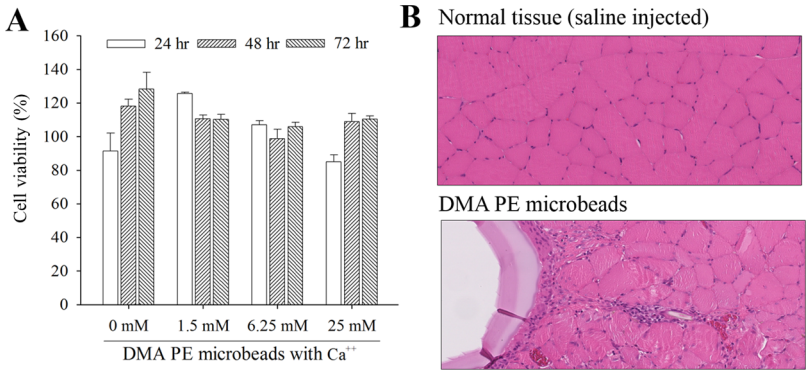

Figure 6. Cellular toxicity and tissue compatibility of DMA PE microbeads. (A) Viability of MC3T3-E1 preosteoblast cells after treatment with DMA PE microbeads. (B) Histological observation of rat thigh muscles after injection of normal saline (control) and DMA PE microbeads; muscles were recovered 1 week after the injection and H&E stained.

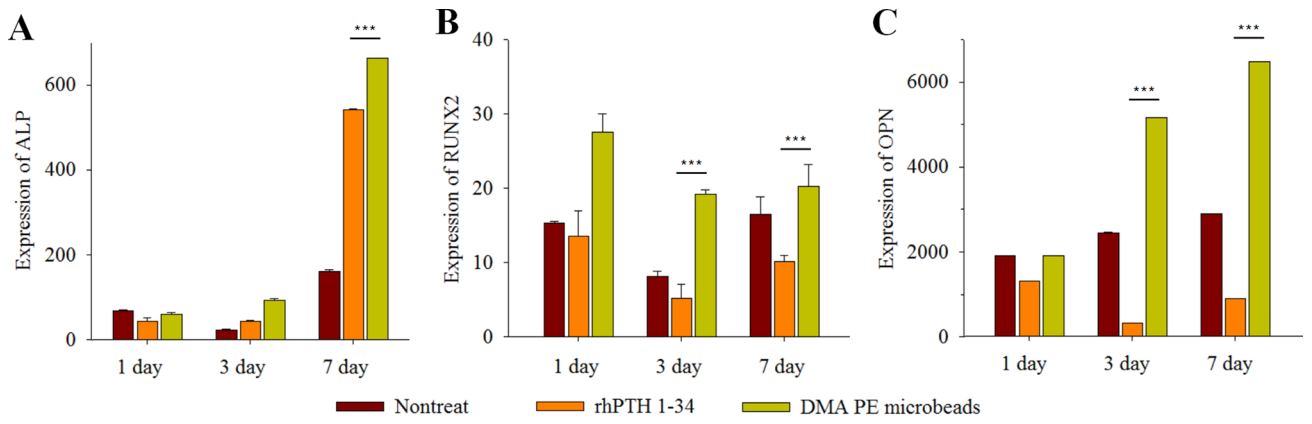

Figure 7. Relative expression of bone formation markers. MC3T3-E1 cells were treated with rhPTH 1-34 released from DMA PE microbeads under pulsatile-treated Ca^{2+} triggering and subjected to PCR study together with nontreated cells and continuous rhPTH1-34 treated cells. (A) Relative expression of alkaline phosphatase (ALP). (B) Relative expression of runt-related transcriptase factor 2 (RUNX2). (C) Relative expression of osteopontin (OPN). Experiments were performed in triplicate (mean ± S.D., *** $P < 0.001$).

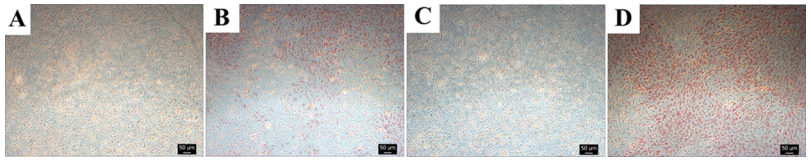

Figure 8. Mineral disposition of OCCM-30 cells: (A) nontreated, (B) rhPTH1-34 treated, (C) blank DMA PE microbeads, and (D) rhPTH1-34 loaded DMA PE microbeads treated under pulsatile Ca^{2+} triggering, respectively. Cells were stained with Alizalin Red S.

upregulated in most groups. However, the expression was prominently increased in the DMA PE microbeads group. The expression of RUNX2 in the early stage of differentiation increased more on day 1 than other days. RUNX2 was upregulated by 51% in the pulsatile drug release group compared with the continuous drug release group. The expression of ALP in the middle stage of differentiation dramatically increased on day 7. OPN increased continuously from day 0 to day 7. The expression of OPN significantly increased (by 94%) on day 3 in the pulsatile drug release group compared with the continuous drug release group.

3.6. Mineralized Nodule Formation. Alizarin red S staining is widely used to evaluate cellular disposition of calcium and verifies whether bone formation markers resulted in a mineralized nodule formation. OCCM-30 cells were incubated with DMA PE microbeads with/without rhPTH 1-34 for 10 days and stained with alizarin red S. As shown in Figure 8, the control cells and cells treated with DMA PE without rhPTH 1-34 were not stained by alizarin red S. This indicated that there was no disposition of minerals. However, in the case of cells treated with DMA PE microbeads loaded with rhPTH 1-34, >80% were densely stained with the dye. These results suggested that the OCCM-30 cells were activated by rhPHT 1-34 released in a pulsatile manner from microbeads. Moreover, the in vitro cellular study proved that the pulsatile release of rhPTH 1-34 induced bone formation markers of ALP, RUNX2, and OPN in preosteoblast cells (MC3T3-E1), whereas the continuous delivery of rhPTH 1-34 did not result in the induction of bone formation markers. These results correspond with the mineralized nodule formation study. Although further studies are required to demonstrate possible interference with other cationic ions in the body, we propose that the bone resorption by osteoclasts increases the local concentration of

DOI: 10.1021/acs.biomac.7b00750
Biomacromolecules 2017, 18, 3099−3105

free Ca^{2+} ions, which triggers the release of rhPTH 1-34 from DMA PE microbeads and enhances the activity of osteoblasts.

4. CONCLUSIONS

We developed a simple fabrication method for anionic polyelectrolyte microbeads using microfluidic photopolymerization and demonstrated its potential in the pulsatile delivery of rhPTH 1-34. One anionic polyelectrolyte microbead actively absorbed up to 23.4 ± 0.9 μg of the cationic rhPTH 1-34 and released it in a pulsatile manner in response to Ca^{2+} ions. The pulsatile release stimulated the expression of bone formation markers and mineral disposition in osteoblasts. Our experimental data support that polyelectrolyte microbeads can be used as a rhPTH 1-34 carrier in the treatment of osteoporosis.

■ ASSOCIATED CONTENT

Supporting Information

The Supporting Information is available free of charge on the ACS Publications website at DOI: 10.1021/acs.biomac.7b00750.

^{1}H NMR, FT-IR spectra of polyelectrolyte microbeads, and table of gene sequences used in this study. (PDF)

■ AUTHOR INFORMATION

Corresponding Author

*Tel: +82-32-890-2382. Fax: +82-32-890-1199. E-mail: sugeun.yang@inha.ac.kr.

ORCID

Su-Geun Yang: 0000-0001-5278-8723

Author Contributions

#M.K.K. and H.N.L. equally contributed to this research.

Notes

The authors declare no competing financial interest.

■ ACKNOWLEDGMENTS

This research was supported by Basic Science Research Program through the National Research Foundation of Korea (NRF) funded by the Ministry of Science, ICT, and Future Planning (NRF-2017R1A2A2A07001272) as well as by WCSL (World Class Smart Lab) research grant from Inha University.

■ REFERENCES

(1) Black, D. M.; Rosen, C. J. Clinical Practice. Postmenopausal Osteoporosis. *N. Engl. J. Med.* **2016**, *374*, 254−62.

(2) Neer, R. M.; Arnaud, C. D.; Zanchetta, J. R.; Prince, R.; Gaich, G. A.; Reginster, J. Y.; Hodsman, A. B.; Eriksen, E. F.; Ish-Shalom, S.; Genant, H. K.; Wang, O.; Mitlak, B. H.; et al. Effect of parathyroid hormone (1-34) on fractures and bone mineral density in postmenopausal women with osteoporosis. *N. Engl. J. Med.* **2001**, *344*, 1434−41.

(3) Chiang, C. Y.; Zebaze, R. M.; Ghasem-Zadeh, A.; Iuliano-Burns, S.; Hardidge, A.; Seeman, E. Teriparatide improves bone quality and healing of atypical femoral fractures associated with bisphosphonate therapy. *Bone* **2013**, *52*, 360−5.

(4) Dobnig, H.; Turner, R. T. Evidence that intermittent treatment with parathyroid hormone increases bone formation in adult rats by activation of bone lining cells. *Endocrinology* **1995**, *136*, 3632−8.

(5) Locklin, R. M.; Khosla, S.; Turner, R. T.; Riggs, B. L. Mediators of the biphasic responses of bone to intermittent and continuously administered parathyroid hormone. *J. Cell. Biochem.* **2003**, *89*, 180−90.

(6) Farra, R.; Sheppard, N. F., Jr.; McCabe, L.; Neer, R. M.; Anderson, J. M.; Santini, J. T., Jr.; Cima, M. J.; Langer, R. First-in-human testing of a wirelessly controlled drug delivery microchip. *Sci. Transl. Med.* **2012**, *4*, 122ra21.

(7) Schanze, K. S.; Shelton, A. H. Functional Polyelectrolytes. *Langmuir* **2009**, *25*, 13698−13702.

(8) Michaels, A. S.; Miekka, R. G. Polycation-polyanion complexes: preparation and properties of poly-(vinylbenzyltrimethylammonium) poly-(styrenesulfonate). *J. Phys. Chem.* **1961**, *65*, 1765−1773.

(9) Costa, R. R.; Mano, J. F. Polyelectrolyte multilayered assemblies in biomedical technologies. *Chem. Soc. Rev.* **2014**, *43*, 3453−79.

(10) Meng, X.; Perry, S. L.; Schiffman, J. D. Complex Coacervation: Chemically Stable Fibers Electrospun from Aqueous Polyelectrolyte Solutions. *ACS Macro Lett.* **2017**, *6*, 505−511.

(11) Serra, V. V.; Teixeira, R.; Andrade, S. M.; Costa, S. M. Design of polyelectrolyte core-shells with DNA to control TMPyP binding. *Colloids Surf., B* **2016**, *146*, 127−135.

(12) Kurinomaru, T.; Shiraki, K. Aggregative protein-polyelectrolyte complex for high-concentration formulation of protein drugs. *Int. J. Biol. Macromol.* **2017**, *100*, 11.

(13) Wang, B.; Jin, T.; Xu, Q.; Liu, H.; Ye, Z.; Chen, H. Direct Loading and Tunable Release of Antibiotics from Polyelectrolyte Multilayers To Reduce Bacterial Adhesion and Biofilm Formation. *Bioconjugate Chem.* **2016**, *27*, 1305−13.

(14) Shukla, P.; Gupta, G.; Singodia, D.; Shukla, R.; Verma, A. K.; Dwivedi, P.; Kansal, S.; Mishra, P. R. Emerging trend in nano-engineered polyelectrolyte-based surrogate carriers for delivery of bioactives. *Expert Opin. Drug Delivery* **2010**, *7*, 993−1011.

(15) He, W.; Parowatkin, M.; Mailander, V.; Flechtner-Mors, M.; Graf, R.; Best, A.; Koynov, K.; Mohr, K.; Ziener, U.; Landfester, K.; Crespy, D. Nanocarrier for Oral Peptide Delivery Produced by Polyelectrolyte Complexation in Nanoconfinement. *Biomacromolecules* **2015**, *16*, 2282−7.

(16) Khemtong, C.; Kessinger, C. W.; Ren, J.; Bey, E. A.; Yang, S. G.; Guthi, J. S.; Boothman, D. A.; Sherry, A. D.; Gao, J. In vivo off-resonance saturation magnetic resonance imaging of alphavbeta3-targeted superparamagnetic nanoparticles. *Cancer Res.* **2009**, *69*, 1651−8.

(17) Levesque, S. G.; Lim, R. M.; Shoichet, M. S. Macroporous interconnected dextran scaffolds of controlled porosity for tissue-engineering applications. *Biomaterials* **2005**, *26*, 7436−7446.

(18) Chen, F. M.; Zhao, Y. M.; Zhang, R.; Jin, F.; Wu, Z. F.; Jin, Y. Novel composite nanoparticles based on glycidyl methacrylate-derivatized dextrans and gelatin as new bone morphogenetic protein carrier. *J. Biomed. Mater. Res., Part A* **2008**, *84A*, 568.

(19) Zanelli, J. M.; Kent, J. C.; Rafferty, B.; Nissenson, R. A.; Nice, E. C.; Capp, M. W.; O'Hare, M. J. High-performance liquid chromatographic methods for the analysis of human parathyroid hormone in reference standards, parathyroid tissue and biological fluids. *J. Chromatogr., Biomed. Appl.* **1983**, *276*, 55−68.

(20) Wainwright, M. The use of dyes in modern biomedicine. *Biotech. Histochem.* **2003**, *78*, 147−55.

(21) Ratanajanchai, M.; Lee, D. H.; Sunintaboon, P.; Yang, S. G. Photo-cured PMMA/PEI core/shell nanoparticles surface-modified with Gd-DTPA for T1MR imaging. *J. Colloid Interface Sci.* **2014**, *415*, 70−6.

(22) Estebanez, P.; Sarasqueta, C.; Najera, R.; Contreras, G.; Perez, L.; Fitch, K.; Vicente, A. Prevalence of HIV-1, HIV-2, and HTLV-I/II in Spanish seamen. *JAIDS, J. Acquired Immune Defic. Syndr.* **1992**, *5*, 316−7.

DOI: 10.1021/acs.biomac.7b00750
Biomacromolecules 2017, 18, 3099−3105